

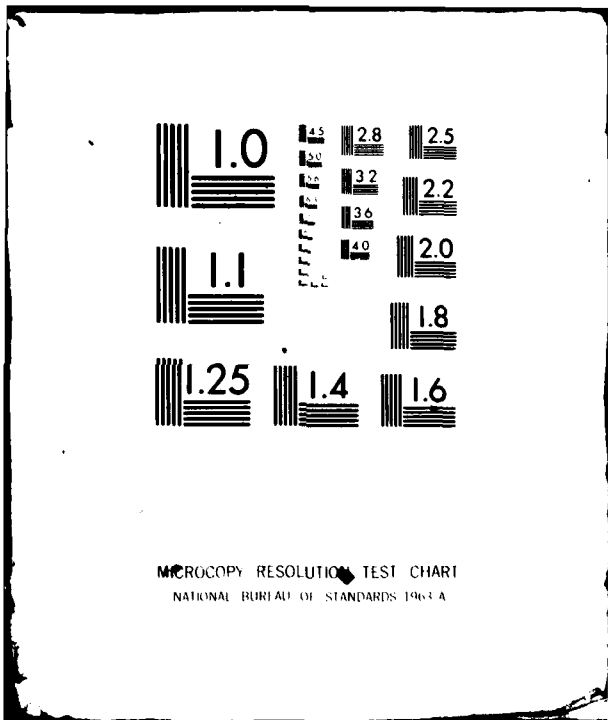
AD-A086 784

NAVAL RESEARCH LAB WASHINGTON DC F/6 20/9  
HARD X-RAY SPECTRUM FROM A ONE-FLUID LASER PLASMA MODEL.(U)  
MAY 80 D G COLOMBANT, W M MANHEIMER DE-A108-790P40092  
NRL-MR-4241 SBIE-AD-E000 463 NL

UNCLASSIFIED

1 - 1  
20  
2000-10-13

END  
DATE  
FILMED  
8 80  
DTIC



MICROCOPY RESOLUTION TEST CHART  
NATIONAL BUREAU OF STANDARDS 1963-A

ADA 086784

UNCLASSIFIED

SECURITY CLASSIFICATION OF THIS PAGE (When Data Entered)

REPORT DOCUMENTATION PAGE		READ INSTRUCTIONS BEFORE COMPLETING FORM
1. REPORT NUMBER NRL Memorandum Report 4241	2. GOVT ACCESSION NO. AD-A086 784	3. RECIPIENT'S CATALOG NUMBER
4. TITLE (and Subtitle) HARD X-RAY SPECTRUM FROM A ONE-FLUID LASER PLASMA MODEL		5. TYPE OF REPORT & PERIOD COVERED Interim report on a continuing NRL problem.
7. AUTHOR(s) D.G. Colombant and W.M. Manheimer		6. PERFORMING ORG. REPORT NUMBER
9. PERFORMING ORGANIZATION NAME AND ADDRESS Naval Research Laboratory Washington, DC 20375		8. CONTRACT OR GRANT NUMBER(s)
11. CONTROLLING OFFICE NAME AND ADDRESS U.S. Department of Energy Washington, DC 20545		10. PROGRAM ELEMENT, PROJECT, TASK AREA & WORK UNIT NUMBERS DE-A108-79DP40092 67-0859-0-0
14. MONITORING AGENCY NAME & ADDRESS (if different from Controlling Office) 12-15		16. REPORT DATE May 20 1980
		17. NUMBER OF PAGES 14
		18. SECURITY CLASS. (of this report) UNCLASSIFIED
		18a. DECLASSIFICATION/DOWNGRADING SCHEDULE
16. DISTRIBUTION STATEMENT (of this Report) Approved for public release; distribution unlimited. 14 NRL-MR-4241		
17. DISTRIBUTION STATEMENT (of the abstract entered in Block 20, if different from Report) 18 SBIE 19 AD-E000 465		
18. SUPPLEMENTARY NOTES		
19. KEY WORDS (Continue on reverse side if necessary and identify by block number) Laser produced plasmas Hard x-rays Electron temperature Heat-flux limit 10 to the 15th power W/sq cm.		
20. ABSTRACT (Continue on reverse side if necessary and identify by block number) P Comparisons between hard x-ray experimental spectra and those obtained from a one-dimensional, one-temperature fluid laser-produced plasma model show good agreement over several orders of magnitude in x-ray intensity and for Nd-laser irradiances varying between 1 and $8 \times 10^{15}$ W/cm <sup>2</sup> . The key to this agreement is the careful modeling of electron energy flux limitation by return current driven ion acoustic turbulence. X		

DD FORM 1 JAN 73 1473

EDITION OF 1 NOV 65 IS OBSOLETE  
S/N 0102-LF-014-6601

UNCLASSIFIED

SECURITY CLASSIFICATION OF THIS PAGE (When Data Entered)

251950

CONTENTS

I. INTRODUCTION----- 1

II. MODEL----- 2

III. RESULTS----- 4

IV. CONCLUSION----- 6

V. ACKNOWLEDGEMENT----- 6

REFERENCES----- 7

Accession For	
NTIS GRA&I <input checked="" type="checkbox"/>	
IDC TAB <input type="checkbox"/>	
Unannounced <input type="checkbox"/>	
Justification _____	
By _____	
Distribution/ _____	
Availability Codes	
Dist.	Avail and/or special
A	

DTIC  
ELECTE  
S JUL 17 1980 D  
D

## HARD X-RAY SPECTRUM FROM A ONE-FLUID LASER PLASMA MODEL

### I. Introduction

The space-time integrated experimental x-ray spectra obtained from laser-produced plasmas typically show a two-temperature structure. The energetic part of the spectrum - which yields the hot temperature  $T_h$  - has been used as supporting evidence for suprathermal electrons<sup>1</sup>, flux inhibition mechanism<sup>2</sup> and self-generated magnetic fields.<sup>3</sup> The first interpretation is however the most common one and relies on the generation of a small suprathermal electron population directly responsible for the energetic X rays. This population is assumed to coexist everywhere with the bulk of the electrons which are much cooler and which give rise to the cold temperature  $T_c$  in the x-ray spectrum.

Generally in presenting hard x-ray data, lines are drawn through experimental points which show sharp breaks in the curve. These breaks are used to justify the coexistence of two electron temperatures everywhere. However, we should note that a) some of these kinks occur even at relatively small energy (below 10 keV) and b) often smooth curves can be drawn through the error bars which fit the data as well as kinked curves.

We show on various specific cases that in accordance with ref. 2 and 3 for example, it is also possible to interpret the data in terms of a single-temperature electron fluid. One of the differences between a one-temperature and a multi-group treatment of the electrons is that it is easier to fit an experimental curve with a multi-group treatment since

Manuscript submitted April 10, 1980

several parameters (for instance temperature, number of hot electrons and flux limit for each energy bin) have to be included into the multi-group model. In a fluid model, all the electrons become very hot for a short period of time, in a very localized region. The basic criterion for this model to hold is that the fluid approach has to be valid. In that case, the mean free path of an electron or its Larmor radius must be smaller than a characteristic length of the plasma (henceforth, we will not consider magnetic fields). For a Nd laser-produced plasma, a characteristic length near the critical density is of order  $1\mu$ .<sup>4</sup> At other places in the plasma, it is at least 10 times as long. The mean free path of a 10 keV electron at the critical density is about 0.2 cm. Thus, for a single fluid theory to be valid, there must be some anomalous process which greatly reduces this mean free path. Our model invokes return current driven ion acoustic turbulence to reduce the mean free path.

In this work, we present calculated x-ray spectra from a one-temperature fluid model. We have calculated these spectra for different energies and we compare them to detailed experimental spectra obtained at the Naval Research Laboratory.<sup>5</sup> Several variations of parameters are investigated and discussed.

## II. Model

The model which has been used in this study has been described in detail before.<sup>6</sup> It is characterized by three different absorption mechanisms, stimulated Brillouin backscattering and heat flux limitation. The three absorption processes are inverse bremsstrahlung, resonant absorption and absorption due to ion acoustic turbulence. This latter process allows the fluid description because of the anomalous collision frequency. In ref. 6,

it has been shown that the mean free path is given roughly by  $v_e / \omega_{pe} (\frac{e\phi}{T_e})^2$  where  $(\frac{e\phi}{T_e})$  is a measure of the ion acoustic fluctuation level. If  $(e\phi/T_e) \sim 10^{-1}$ , the electron mean free path for a 10 keV plasma at  $n = 10^{21} \text{ cm}^{-3}$  is roughly  $2\mu$ , which is comparable to the shortest characteristic length in a Nd-laser produced plasma. Heat flux limitation follows from the same physical mechanism and is included in a self-consistent fashion into the code. Stimulated Brillouin backscatter is also included into the code but does not play a major role in the short pulses considered in this work.

One difference between this work and ref. 6 is the treatment of the dense region behind the absorption region. In the present studies, appreciable amounts of radiation come from this region. Therefore more care was taken in modeling this part of the plasma. Specifically, many more grid cells were included in the high-density region. Also the boundary condition at the high density side was taken to mock up thermal contact with a slab at  $T_e = 100 \text{ eV}$  and also having  $\frac{\partial n}{\partial x} = 0$ ,  $\frac{\partial v}{\partial x} = 0$ , to model free flow of matter and momentum into or out of the slab. Since a one-dimensional model might be inappropriate, we have crudely investigated 2-D effects by assuming that lateral thermal conduction can be modeled by a loss term  $-K/L_c^2 T_e$  in the temperature equation where  $L_c$  is a thermal conduction length and  $K$  is the thermal conduction coefficient. The effects of this length on the results are shown in detail for one case. The free-free radiation was broken into 17 frequency groups going from 700 eV to 100 keV. These groups were not divided evenly over the whole frequency range in order to provide better resolution at the low energy range of the spectrum. The x-ray emission is displayed in erg/keV and corresponds to

radiation emitted in  $4\pi$  steradians. The target is typically a CH planar target with a  $10\mu$  initial characteristic gradient length in front of it (below critical density). The laser pulse is gaussian with 50 psec FWHM and a focal spot radius of  $15\mu$  (the focal spot radius is needed in order to yield absolute radiation levels).

### III. Results

We attempted to reproduce a series of experiments performed at the Naval Research Laboratory<sup>5</sup> in a systematic fashion. This work is then different from any other published work involving one-temperature models because it deals with a whole range of experiments. The experimental data<sup>5</sup> was taken between  $2 \times 10^{14}$  and  $8 \times 10^{15}$  W/cm<sup>2</sup> with a hard x-ray tail appearing above  $7 \times 10^{14}$  W/cm<sup>2</sup>. The numerical results have been obtained for the range 1.5 to  $8 \times 10^{15}$  W/cm<sup>2</sup> for 4 values of the irradiance: 1.5 - 2.5 - 5 and  $8 \times 10^{15}$  W/cm<sup>2</sup>.

No prepulse was present in the experiment and so a  $10\mu$  initial density gradient was assumed in front of the target as in the case of the short pulse simulations in ref. 6. Because of this sharp density gradient, backscattering is not significant.

Before presenting results for the x-ray spectra, let us note that the calculated total absorption varied from a high 43% for the 1.5 J case down to 32% for the 8 J case. Resonant absorption respectively accounted for 27% and 23% for these two cases.

Results and comparisons for the cases mentioned appear in Fig. 1-4. The dotted line for the experimental data below 10 keV represents a best guess since this data was only taken accurately on spherical targets.<sup>5</sup> For the  $1.5 \times 10^{15}$  W/cm<sup>2</sup> case, effects of lateral conduction are shown for

3 different conduction lengths  $L_c = 15\mu$ ,  $50\mu$  and infinite conduction length (no loss is assumed in the radial direction). For the other cases, no radial loss is modeled. For the  $5 \times 10^{15} \text{ W/cm}^2$  case, two numerical x-ray spectra are shown. That one without a hard x-ray tail has been obtained by turning off ion-acoustic turbulence. The lack of a hard x-ray tail in that case can be directly related to the reduced heat flux inhibition since the extra absorption due to ion acoustic turbulence is quite small (39% total absorption compared to 32% when the ion acoustic turbulence is turned off).

As apparent in the various figures, the agreement is quite satisfactory since the difference between numerical and experimental results are at most a factor of 10 over 6 orders of magnitude. Moreover, only a small fraction of the absorbed laser energy can be found in the X rays. Taking into consideration the fact that only the input energy, pulse shape and target material are specified in the numerical model, without any assumption on how much energy is absorbed and/or reflected, we find the agreement quite satisfactory. The hot electron temperature measured from the x-ray spectra between 20 and 90 keV is shown in Fig. 5 for the experiments and for our calculations.

The remarks which can be made on the differences between the theoretical and experimental curves are:

- The numerical curves are smoother than the experimental curves. We have already brought up this point in the introduction.

- The numerical x-ray curves lie above the experimental ones for the low-irradiance case whereas they lie below for the higher irradiance case. It could be that suprathermals near the critical density which increase in

number with irradiance might be necessary to explain the high-irradiance case. Another possible explanation is that the ion acoustic fluctuation level which has been assumed constant does in fact increase with laser irradiance, reducing the electron thermal heat flux and raising the electron temperature.

#### IV. Conclusion

In this work, we have shown that high-energy x-ray spectra can be explained with a one-temperature fluid model which incorporates anomalous transport. The agreement is quite satisfactory over 6 orders of magnitude in x-ray intensity and over a factor of 6 in laser irradiance.

An essential ingredient of the fluid theory is the presence of anomalous collisions which reduce the mean free path of the electrons from their free-streaming value down to a few microns which are characteristic of the scale length in Nd-laser produced plasmas.

#### V. Acknowledgement

We would like to thank Dr. F. Young and B. Ripin for many discussions regarding the experimental data. This work was supported by the Department of Energy.

### References

1. V. W. Slivinsky, H. N. Kornblum and H. D. Shay, J. Appl. Phys. 46, 1973 (1975).
2. R. C. Malone, R. L. McCrory and R. L. Morse, Phys. Rev. Lett. 34, 721 (1975).
3. B. H. Ripin, P. G. Burkhalter, F. C. Young, J. M. McMahon, D. G. Colombant, S. E. Bodner, R. R. Whitlock, D. J. Nagel, D. J. Johnson, N. K. Winsor, C. M. Dozier, R. D. Bleach, J. A. Stamper and E. A. McLean, Phys. Rev. Lett. 34, 1313 (1975).
4. D. Atwood, D. Sweeney, J. Auerbach and P. Lee, Phys. Rev. Lett. 40, 184 (1978).
5. F. C. Young and B. H. Ripin, to be published.
6. D. G. Colombant and W. M. Manheimer, submitted for publication; also NRL Memorandum Report 4083 (1979).

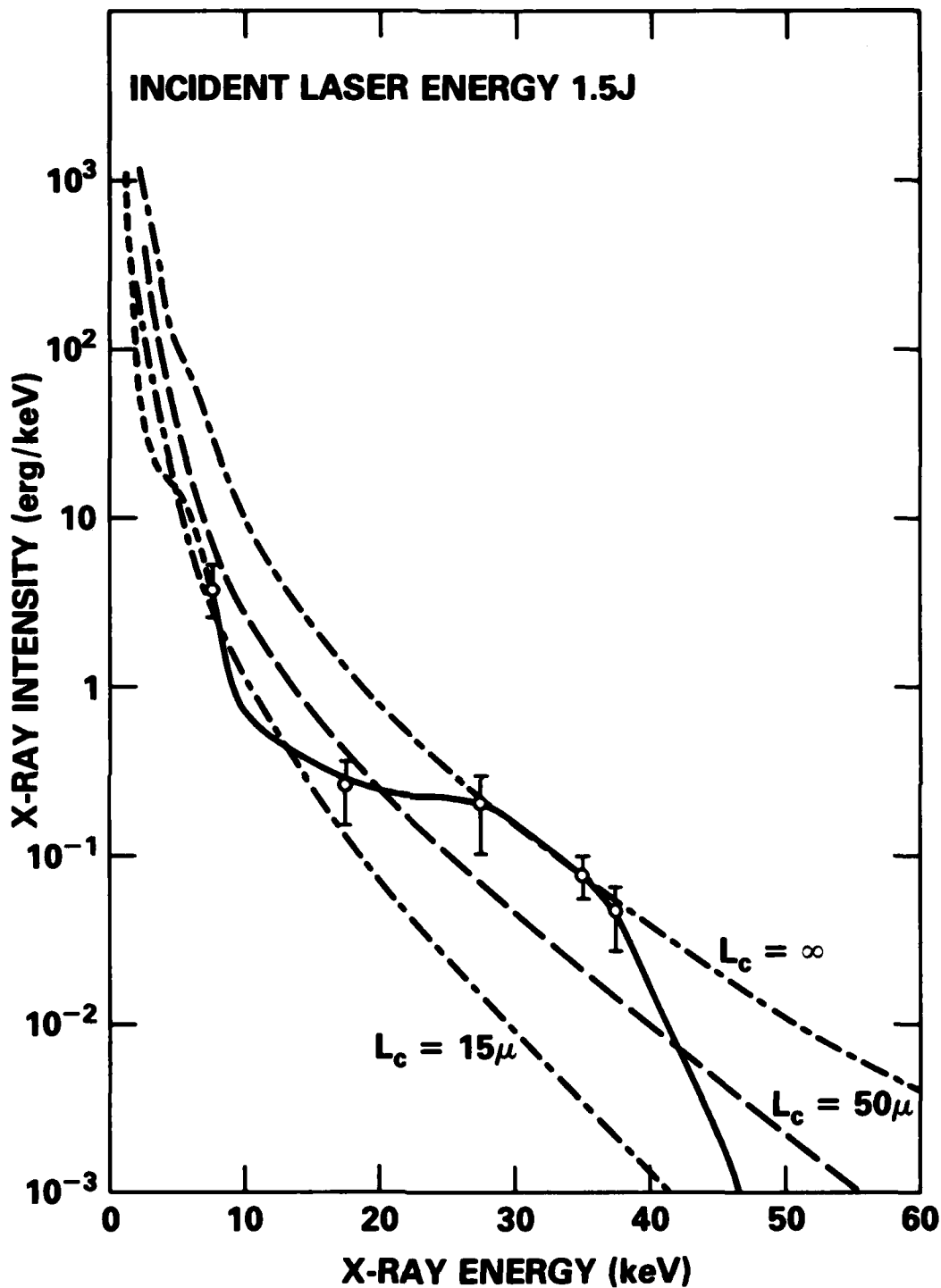


Fig. 1 - Comparison between experimental (solid line) and numerical (dotted line) hard X-ray spectra at  $1.5 \times 10^{15} \text{ W/cm}^2$ . The various numerical spectra correspond to different value of the lateral conduction length  $L_c$ .

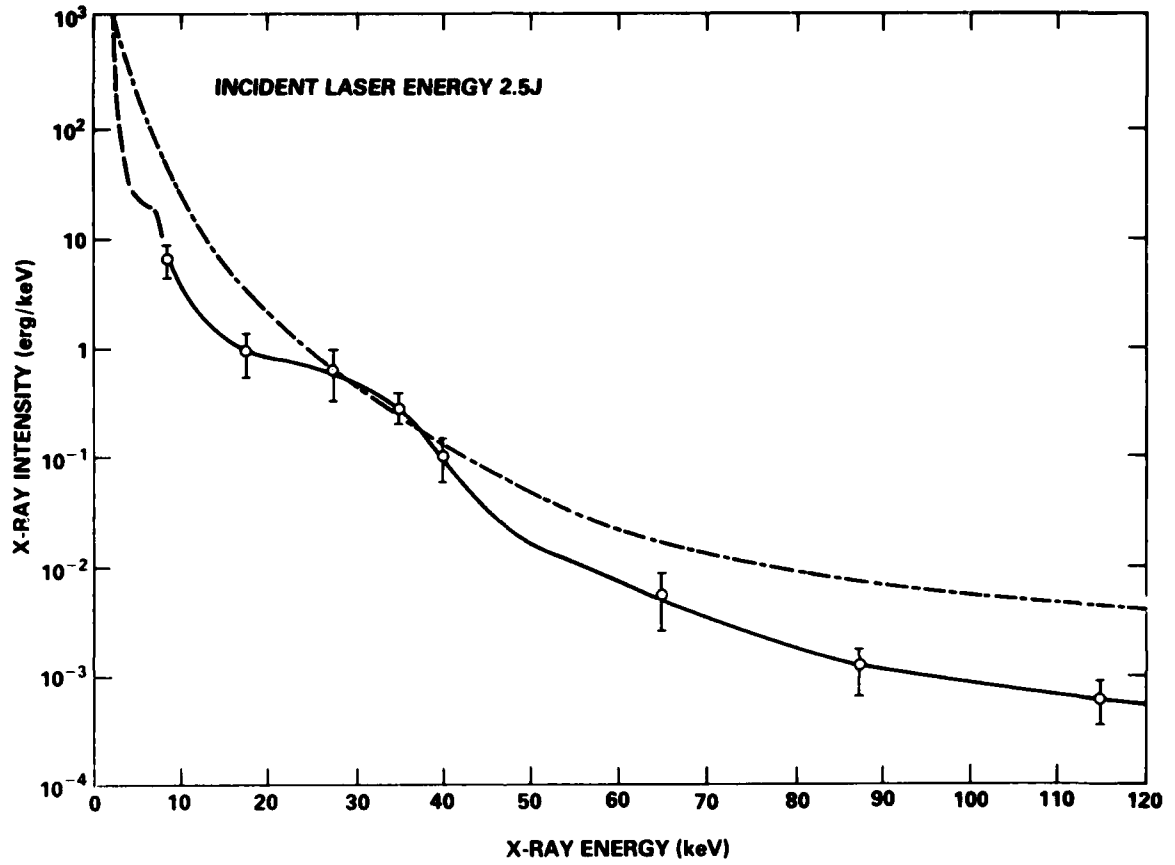


Fig. 2 - Comparison between experimental (solid line) and numerical (dotted line) hard X-ray spectra at  $2.5 \times 10^{15} \text{ W/cm}^2$ . The numerical spectrum has been obtained with no radial loss. Note that for this case, the numerical curve lies above the experimental one.

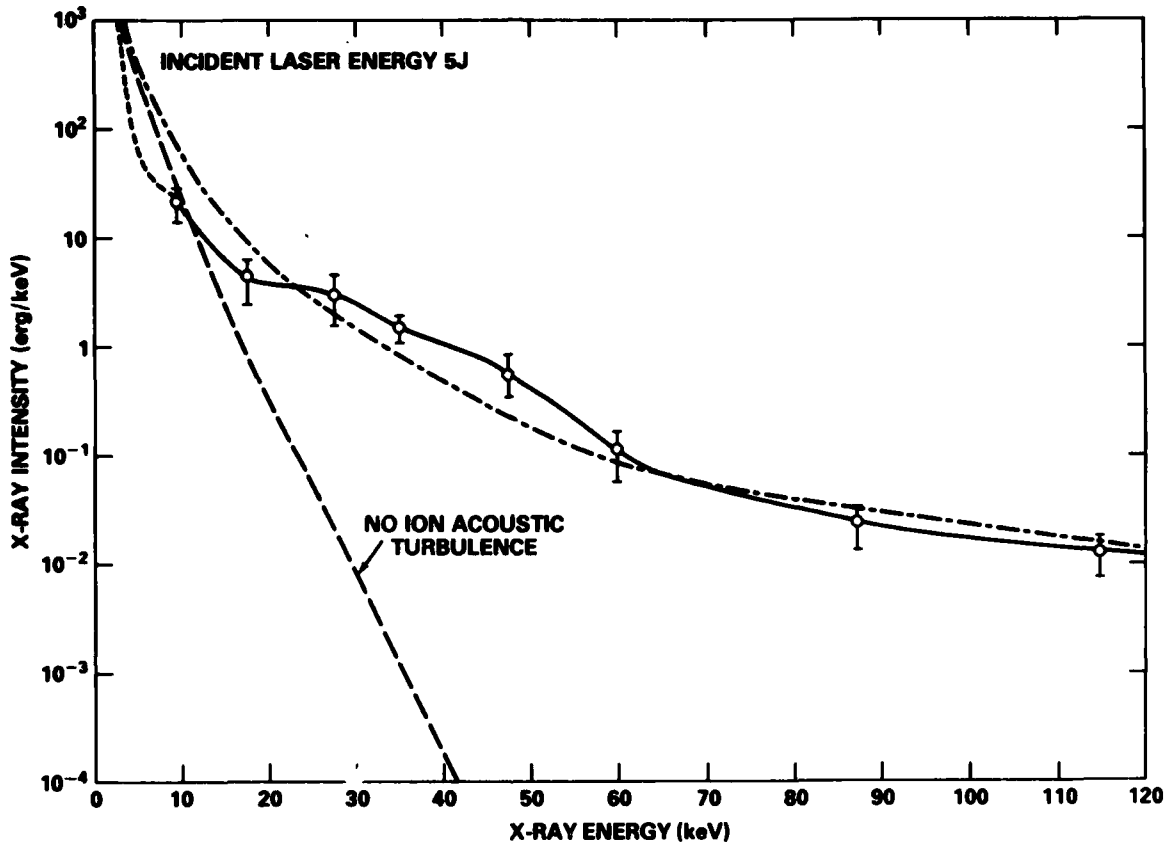


Fig. 3 - Comparison between hard X-ray spectra at  $5 \times 10^{15} \text{ W/cm}^2$ . Note the very good agreement between the experimental (solid line) and the numerical (dotted line) spectra. The numerical curve with the ion acoustic turbulence turned off points out the importance of heat-flux limitation.

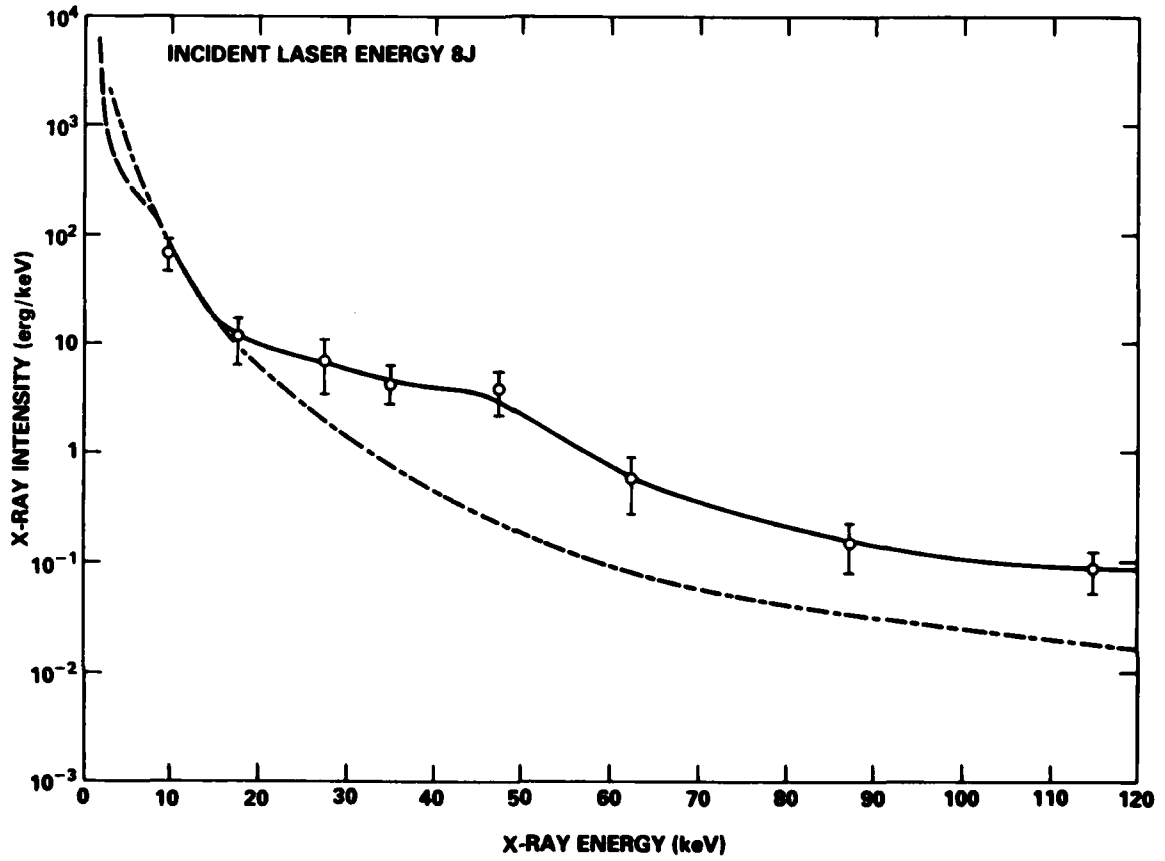


Fig. 4 - Comparison between hard X-ray spectra at  $8 \times 10^{15} \text{ W/cm}^2$ . The numerical curve (dotted line) lies now below the experimental one (solid line).

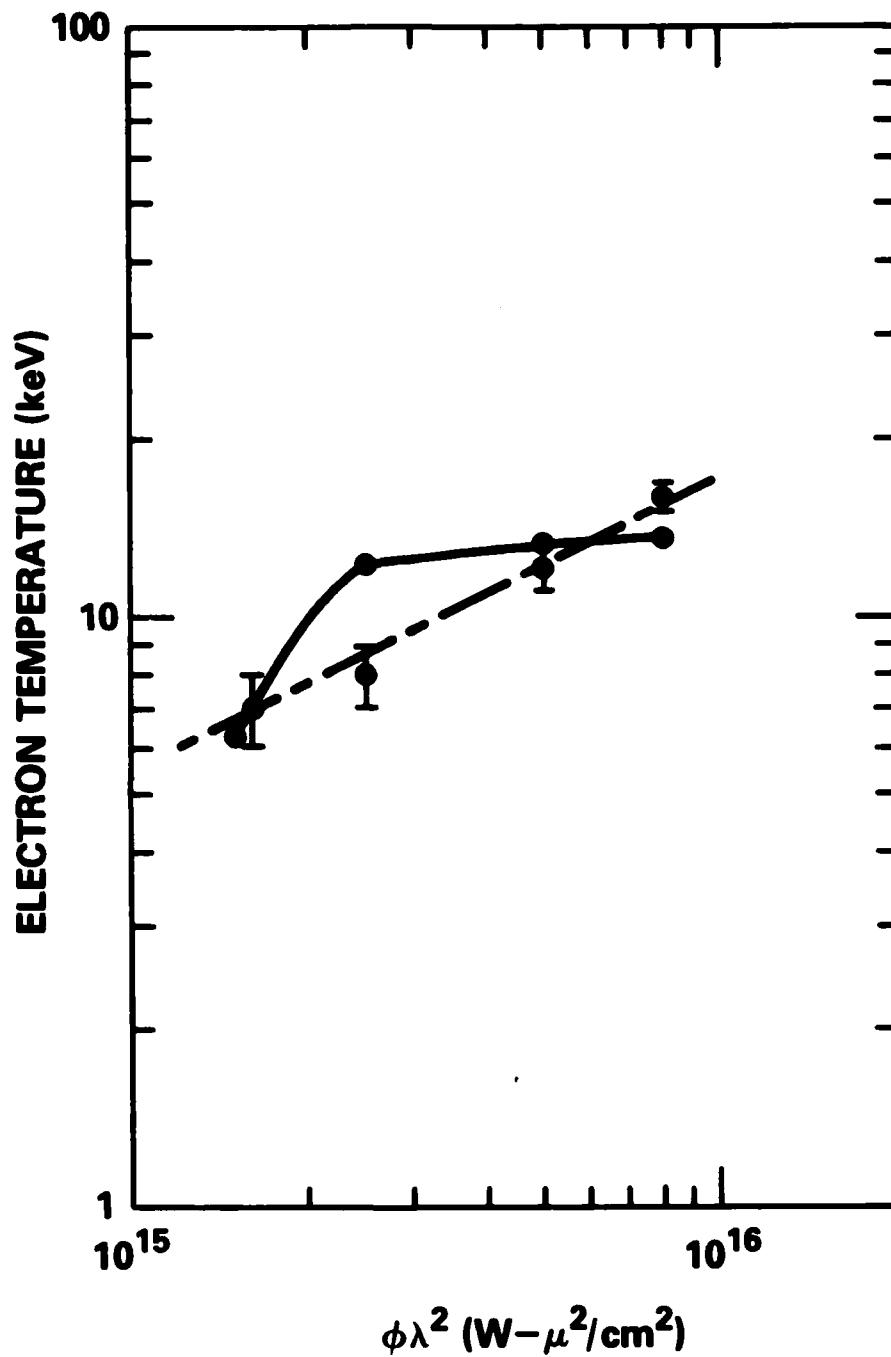


Fig. 5 - Comparison between  $T_h$  derived from the experimental hard X-ray spectra (dotted line) and the numerical spectra (solid line). Except for the point at  $2.5 \times 10^{15} \text{ W}/\text{cm}^2$ , the agreement is very good.

DA  
FILM  
8